Supporting Information

Synergetic antibacterial nanosheet based on $Ti_3C_2T_x$ photothermal therapy and cationic polymer to eradicate drug-resistant bacterial biofilms

Chuming Pang[a], Yingxin Tan[a], Jiahao Ling[a], Liangzhi Hong[a,b*]

[a] School of Materials Science and Engineering, South China University of Technology, Guangzhou 510640, China.

[b] Guangdong Provincial Key Laboratory of Luminescence from Molecular Aggregates, South China University of Technology, Guangzhou 510640, China.

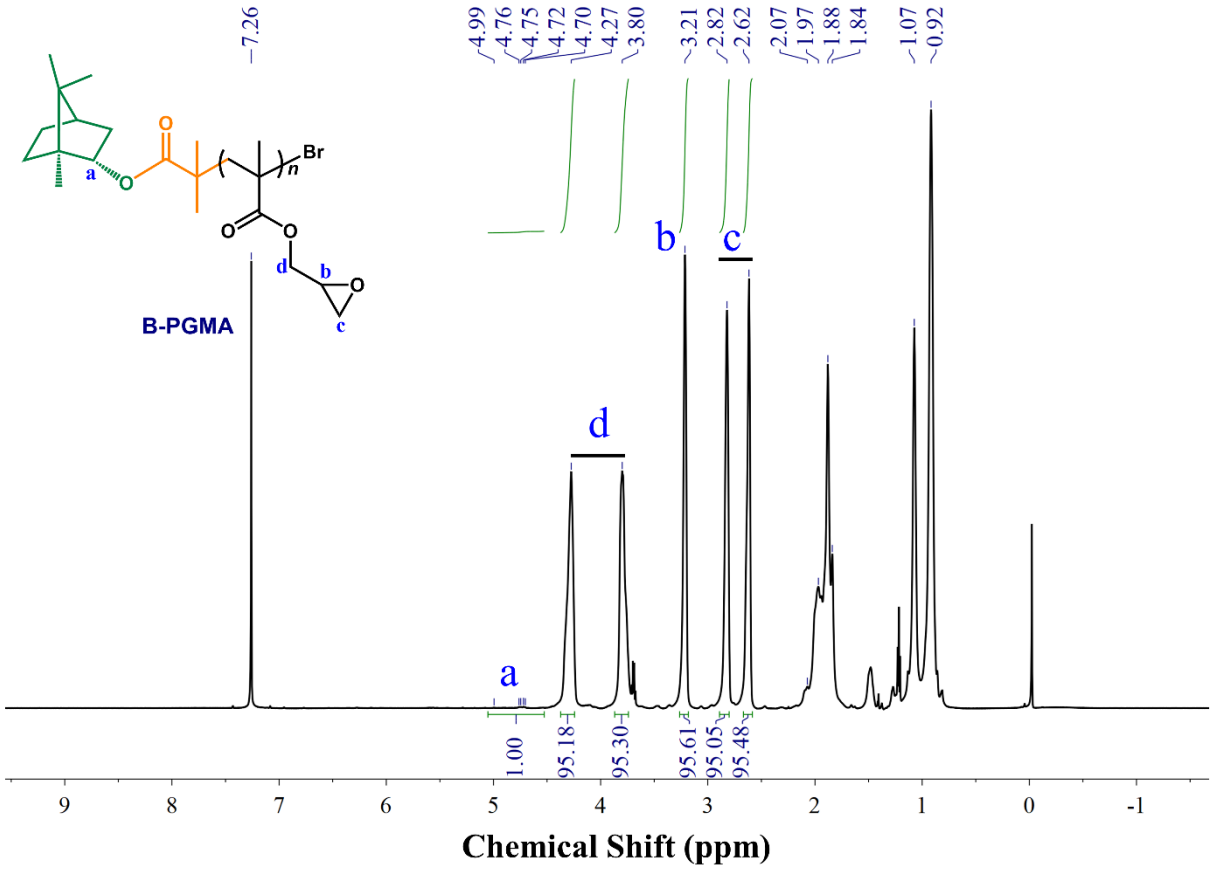

Figure S1 The ^{1}H NMR spectrum (600 MHz, $CDCl_3$) of α-(+)-borneol-poly(glycidyl methacrylate) (B-PGMA).

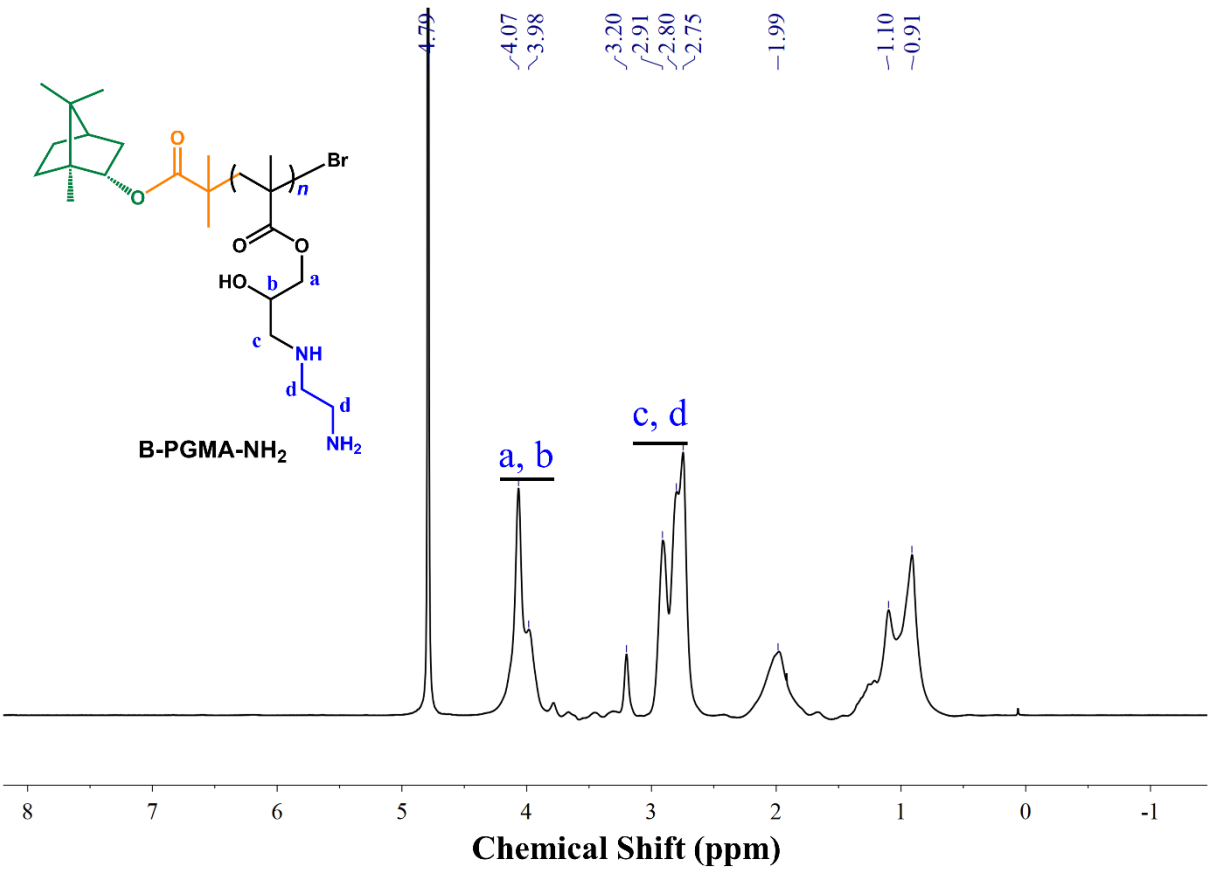

Figure S2 The ^{1}H NMR spectrum (600 MHz, D_2O) of ring-open product primary amine modified α-(+)-borneol-poly(glycidyl methacrylate) (B-PGMA-NH_2).

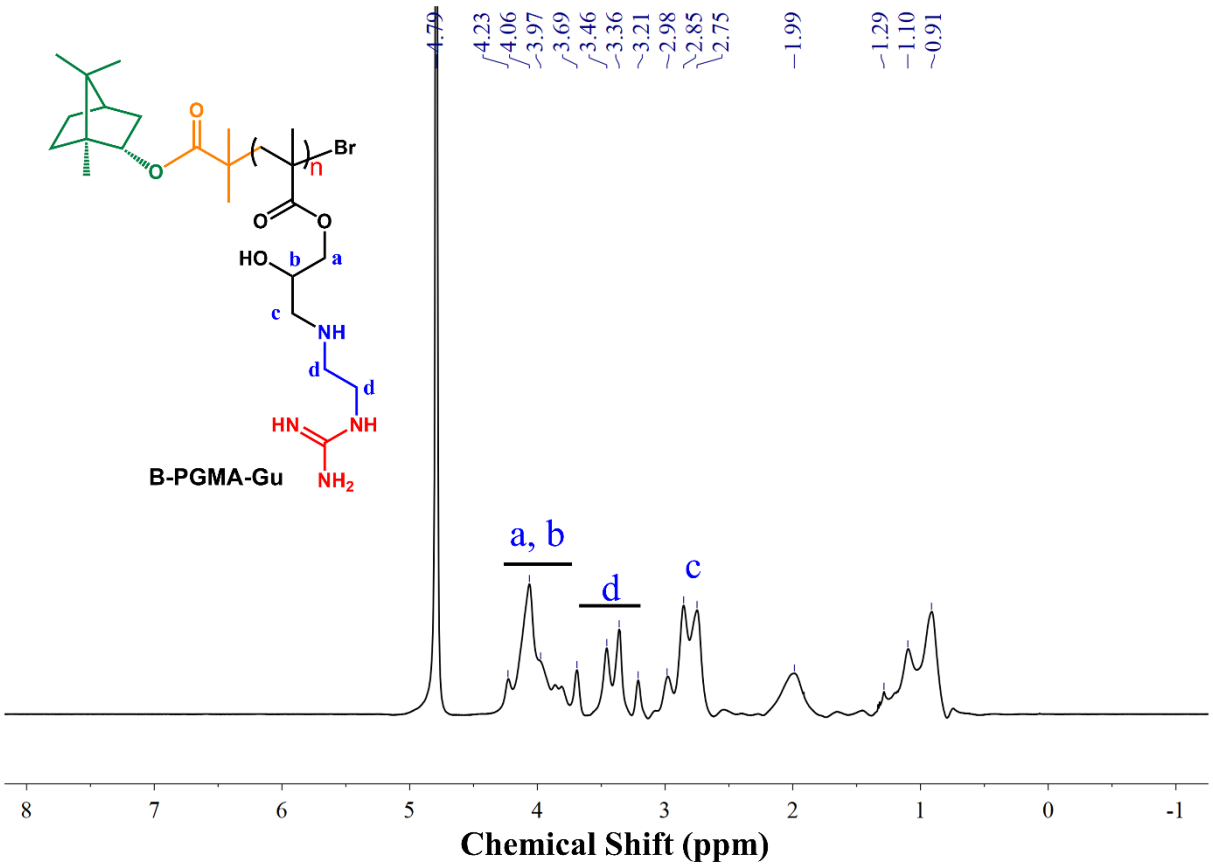

Figure S3 The ^{1}H NMR spectrum (600 MHz, D_2O) of guanidine modified α-(+)-borneol-poly(glycidyl methacrylate) (B-PGMA-Gu).

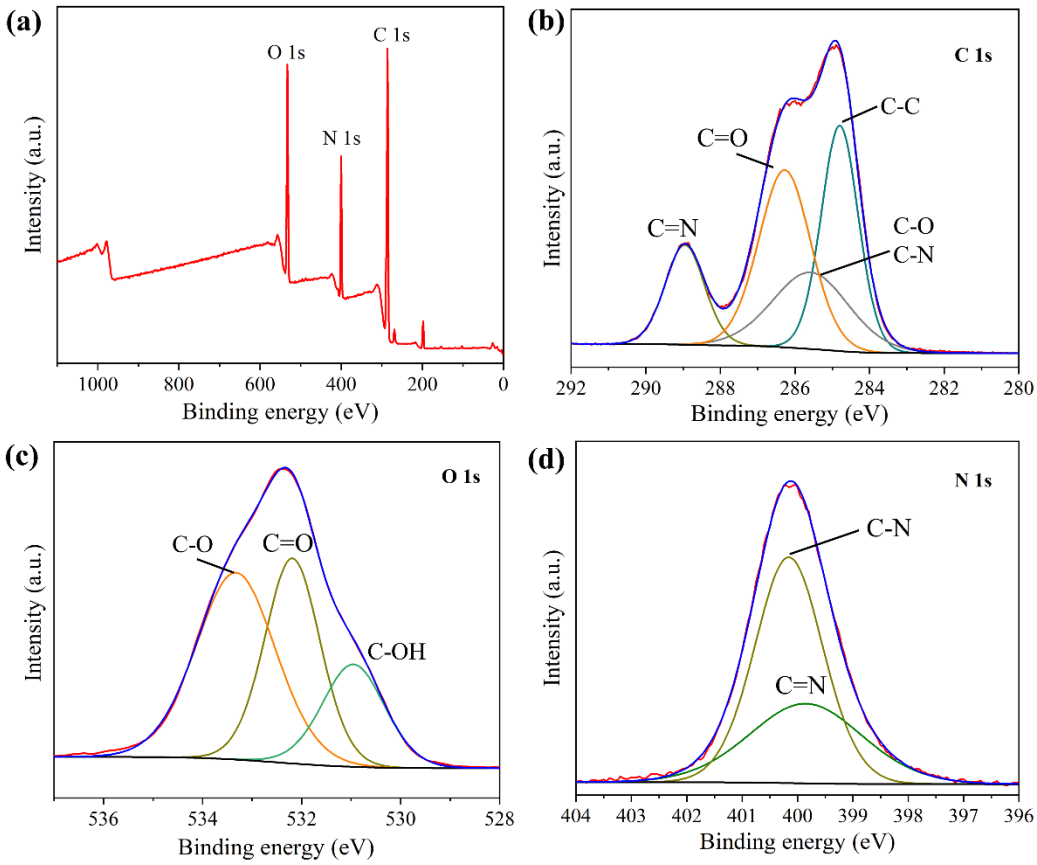

Figure S4 (a-d) The XPS spectra of guanidine-based polymer B-PGMA-Gu and its high-resolution fine spectra.

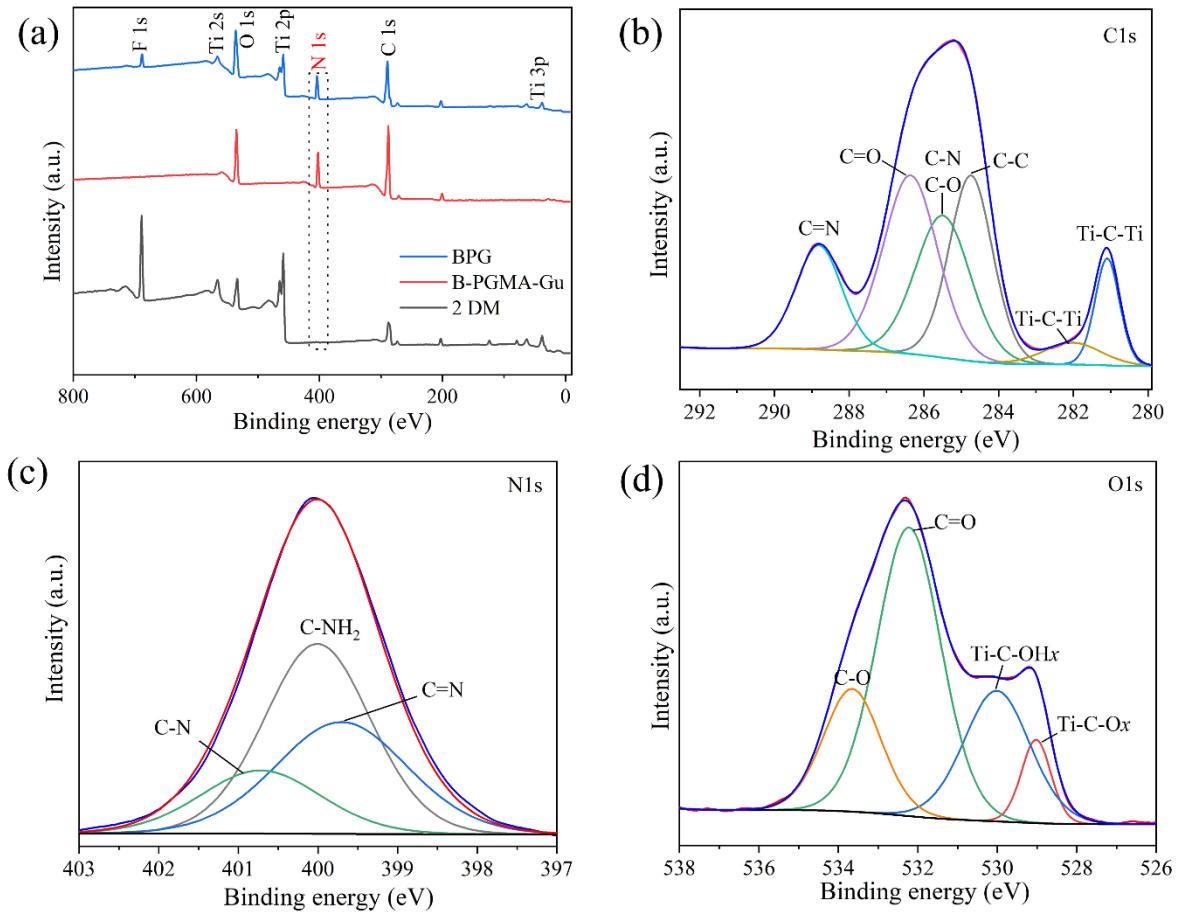

Figure S5 (a-d) The XPS spectra of 2D nanosheet BPG and its high-resolution fine spectra.

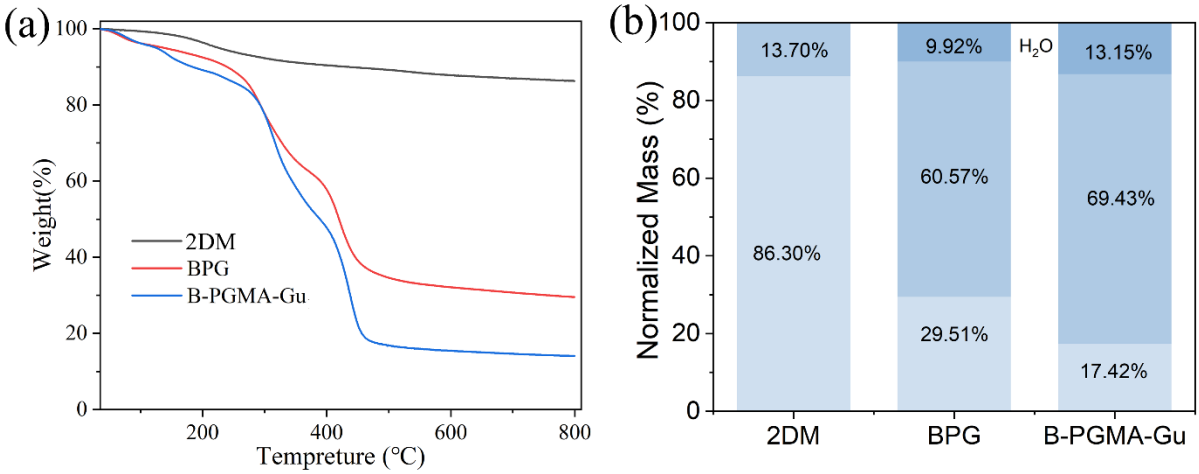

Figure S6 (a) The thermogravimetric analysis (TGA) of BPG, B-PGMA-Gu and 2DM and (b) their normalized weight loss distribution. (Temperature rate: 10 °C·min^{-1}, protective gas: N_2).

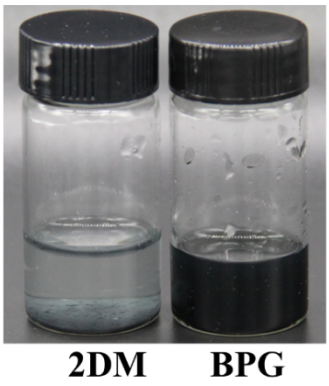

Figure S7 The photo of 2DM and BPG aqueous solution storage at 4 ℃ for 14 days.

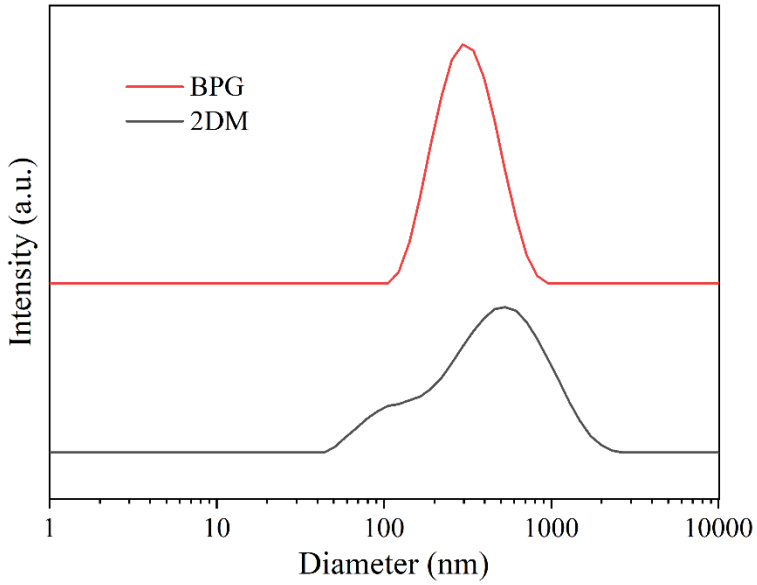

Figure S8 The particle-size distribution of BPG and 2DM in H_2O detected by DLS analysis.

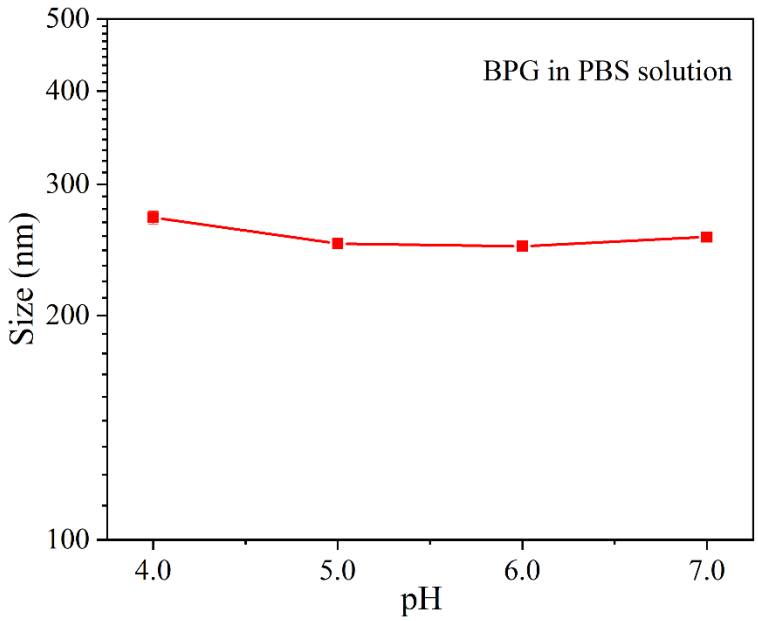

Figure S9 The corresponding diameter changes of BPG in PBS at different pH values.

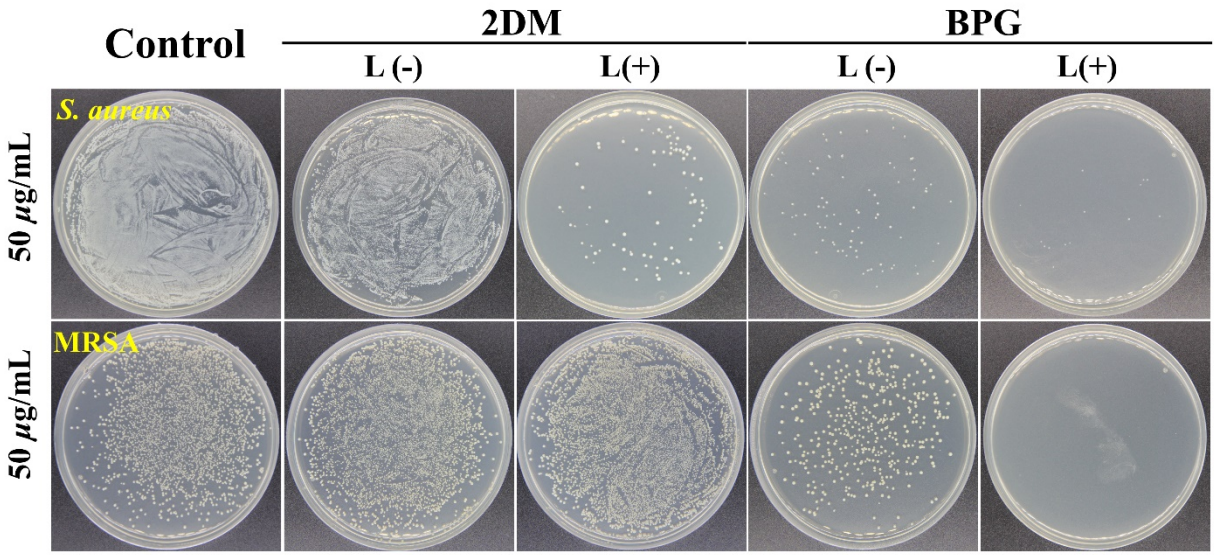

Figure S10 The vitro photothermal antibacterial activity (0.7 W cm^{-2}, 5 min) of composite BPG and 2DM (50 μg mL^{-1}) against *S. aureus* and *MRSA*.

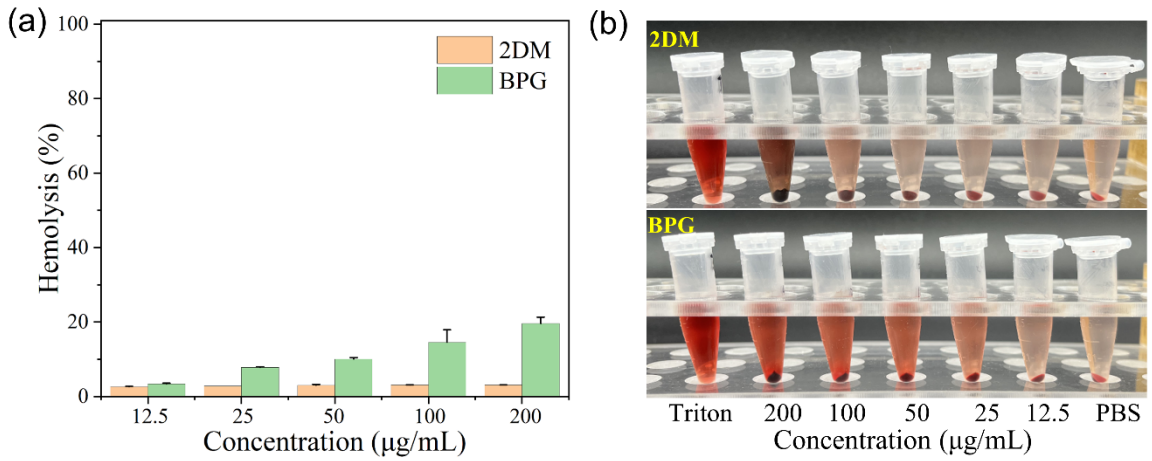

Figure S11 (a) The hemolysis of $Ti_3C_2T_x$ 2DM and BPG at different concentrations and (b) the corresponding photographs of hemolysis.

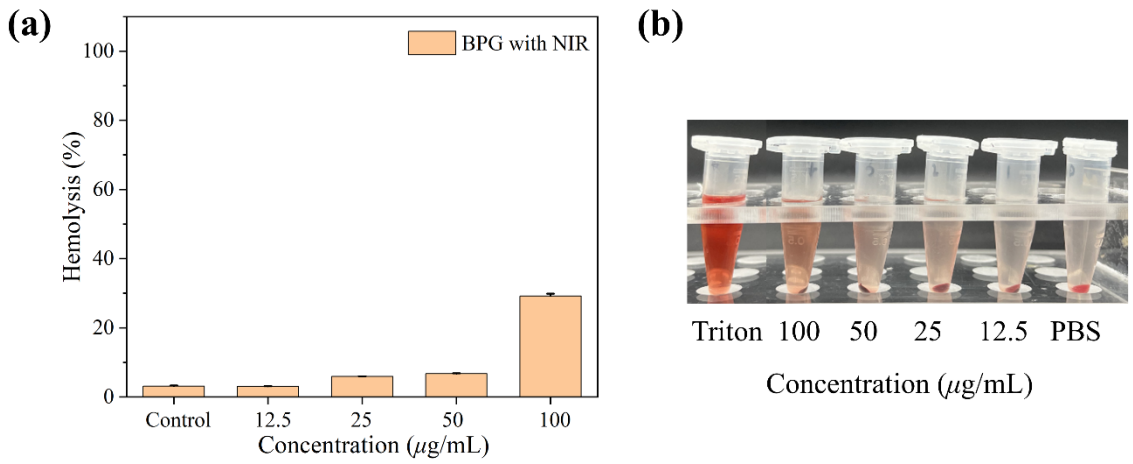

Figure S12 (a) The hemolysis of BPG at different concentrations under 808 nm radiation and (b) the corresponding photographs of hemolysis.

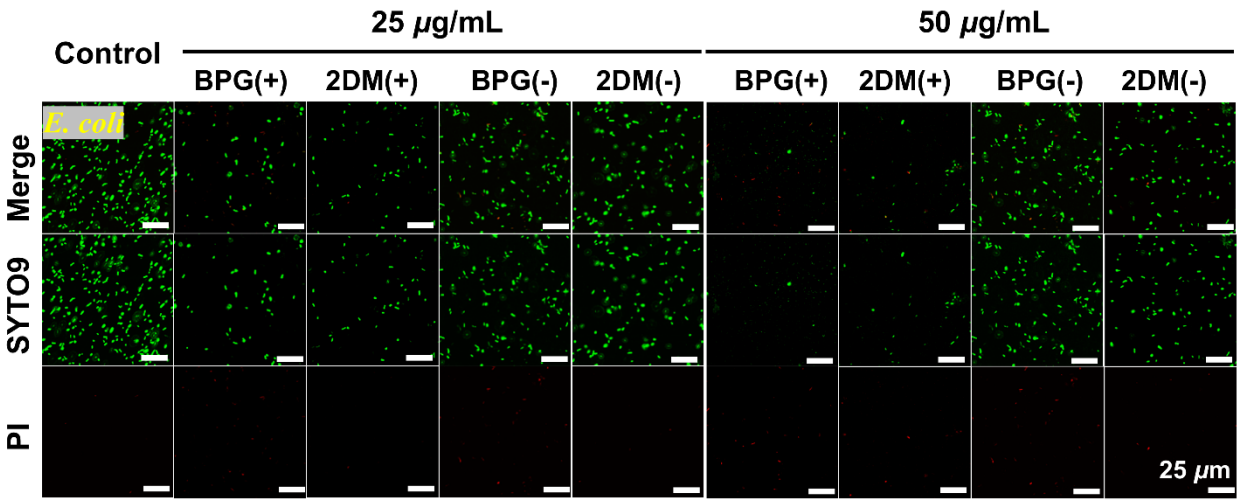

Figure S13 The integrity of cell membrane after the *E. coli* combined with composite BPG or 2DM (c = 25, 50 μg mL^{-1}, (+): with NIR radiation; (-): without NIR radiation).

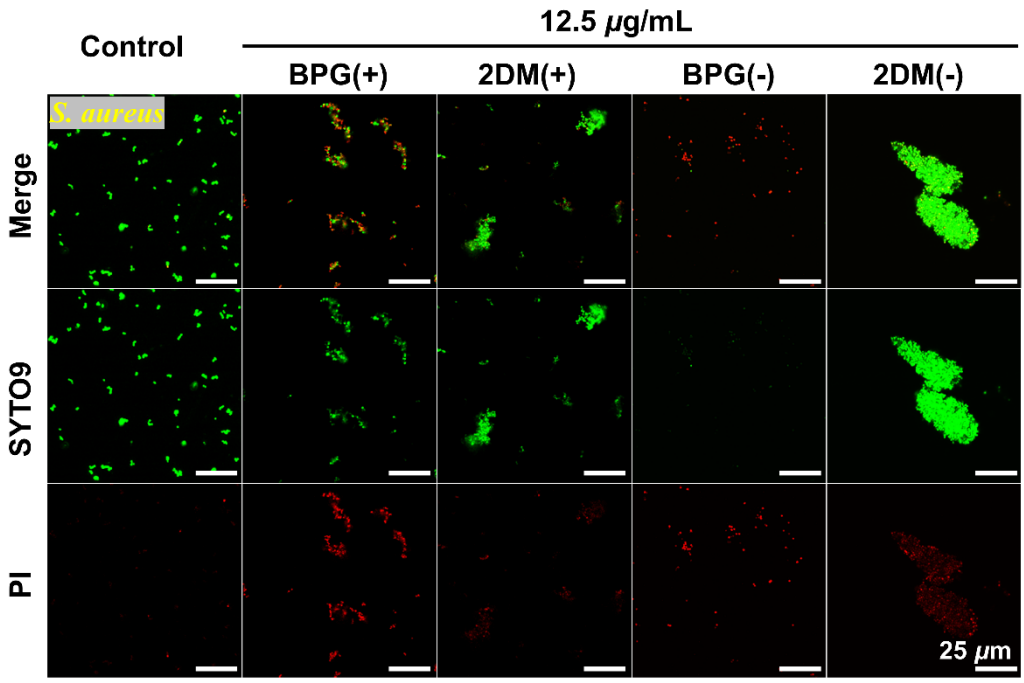

Figure S14 The integrity of cell membrane after the *S. aureus* combined with composite BPG or 2DM (c = 12.5 μg mL^{-1}, (+): with NIR radiation; (-): without NIR radiation).

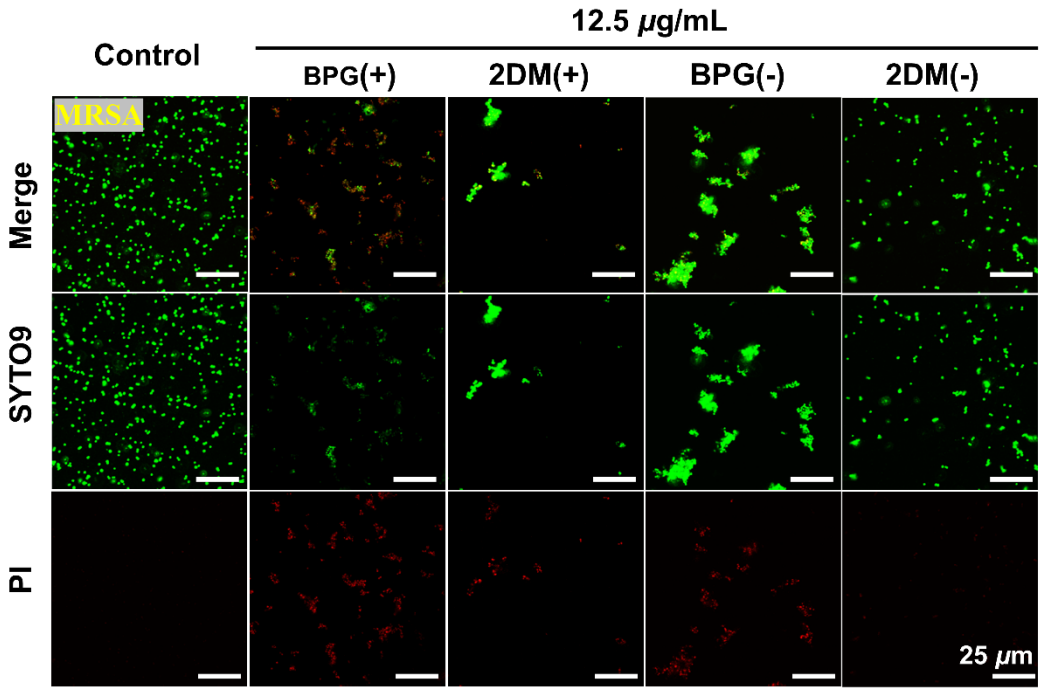

Figure S15 The integrity of cell membrane after the MRSA combined with composite BPG or 2DM (c = 12.5 μg mL^{-1}, (+): with NIR radiation; (-): without NIR radiation).

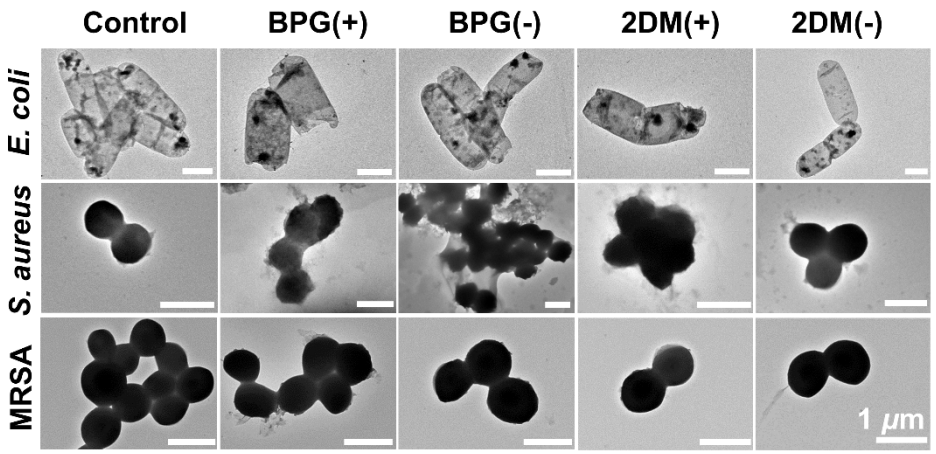

Figure S16 The morphology changes of membrane after treatment with composite BPG or 2DM by TEM analysis.

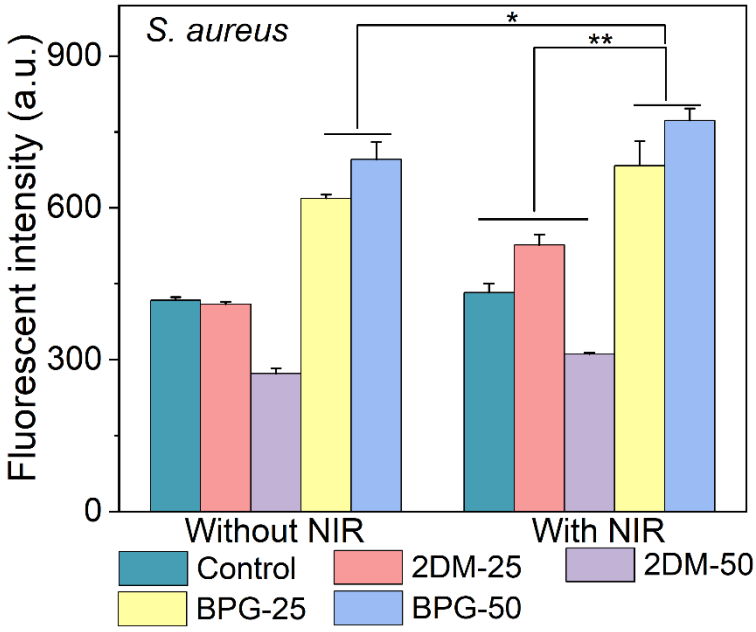

Figure S17 The detection of ROS in the intracellular oxidative stress reaction occurs after *S. aureus* incubated with BPG or 2DM (with/without NIR radiation).

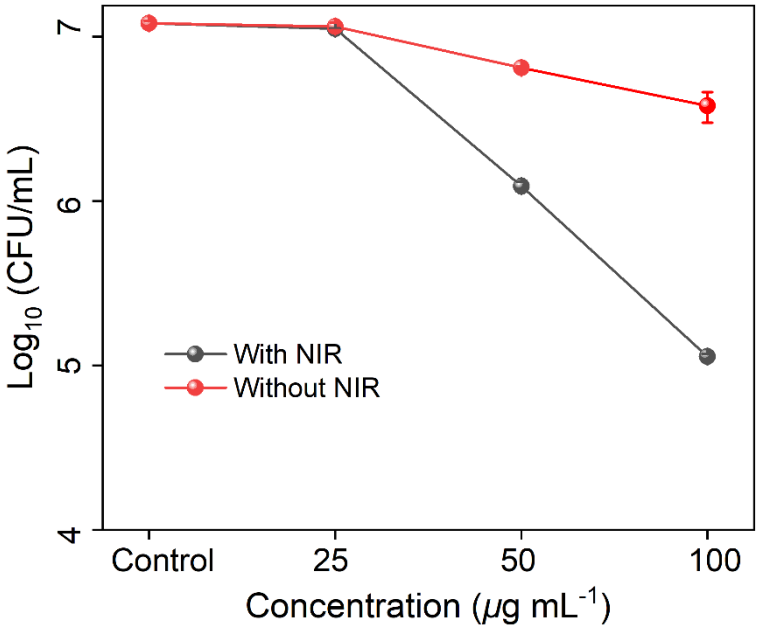

Figure S18 The reduction of bacterial colonies after the mature biofilms treated with different concentrations (25, 50, 100 μg mL^{-1}) of BPG with/without 808 nm NIR radiation.